Multifaceted role of nitric oxide in an *in vitro* mouse neuronal injury model: transcriptomic profiling defines the temporal recruitment of death signalling cascades

Zhao Feng Peng [a, b, #], Minghui Jessica Chen [c, #], Jayapal Manikandan [d], Alirio J. Melendez [d], Guanghou Shui [b], Françoise Russo-Marie [e], Matthew Whiteman [f], Philip M. Beart [g], Philip K. Moore [h, *], Nam Sang Cheung [c, i, *]

[a] *Key Laboratory of Biogeology and Environmental Geology of the Ministry of Education, China University of Geosciences, Wuhan, China*
[b] *Department of Biochemistry, Yong Loo Lin School of Medicine, National University of Singapore, Singapore*
[c] *Menzies Research Institute, University of Tasmania, Hobart, Tasmania, Australia*
[d] *Department of Physiology Yong Loo Lin School of Medicine, National University of Singapore, Singapore*
[e] *Institut Cochin, Paris, France*
[f] *Peninsula Medical School, University of Exeter, St. Luke's Campus, Exeter, Devon, UK*
[g] *Department of Pharmacology, Florey Neurosciences Institutes, University of Melbourne, Parkville, VIC, Australia*
[h] *Pharmaceutical Science Division, King's College, London, UK*
[i] *School of Life and Environmental Sciences, Deakin University, Australia*

Abstract

Nitric oxide is implicated in the pathogenesis of various neuropathologies characterized by oxidative stress. Although nitric oxide has been reported to be involved in the exacerbation of oxidative stress observed in several neuropathologies, existent data fail to provide a holistic description of how nitrergic pathobiology elicits neuronal injury. Here we provide a comprehensive description of mechanisms contributing to nitric oxide induced neuronal injury by global transcriptomic profiling. Microarray analyses were undertaken on RNA from murine primary cortical neurons treated with the nitric oxide generator DETA-NONOate (NOC-18, 0.5 mM) for 8–24 hrs. Biological pathway analysis focused upon 3672 gene probes which demonstrated at least a ± 1.5-fold expression in a minimum of one out of three time-points and passed statistical analysis (one-way ANOVA, $P < 0.05$). Numerous enriched processes potentially determining nitric oxide mediated neuronal injury were identified from the transcriptomic profile: cell death, developmental growth and survival, cell cycle, calcium ion homeostasis, endoplasmic reticulum stress, oxidative stress, mitochondrial homeostasis, ubiquitin-mediated proteolysis, and GSH and nitric oxide metabolism. Our detailed time-course study of nitric oxide induced neuronal injury allowed us to provide the first time a holistic description of the temporal sequence of cellular events contributing to nitrergic injury. These data form a foundation for the development of screening platforms and define targets for intervention in nitric oxide neuropathologies where nitric oxide mediated injury is causative.

Keywords: nitric oxide ● neuronal injury ● oxidative stress ● microarray ● reactive oxygen species ● reactive nitrogen species

[#]Both authors contributed equally to this study.
*Correspondence to: Philip K. MOORE,
University Hall, Lee Kong Chian Wing, UHL Level 5,
National University of Singapore,
21 Lower Kent Ridge Road,
Singapore 119077, Singapore.
Tel.: +65-65163875
Fax: +65-68720830
E-mail: dprmpk@nus.edu.sg

Nam Sang CHEUNG,
Menzies Research Institute,
School of Medicine Private Bag 23,
University of Tasmania,
Hobart, Tasmania 7001, Australia.
Tel.: +613-6226-2710
Fax: +613-6226-7704
E-mail: nscheung@utas.edu.au

Introduction

Nitric oxide, endogenously synthesized in the mammalian system by the nitric oxide synthases (NOS), continues to receive widespread attention for its multifunctional roles in both physiological and patho-physiological conditions. Under physiological conditions, nitric oxide exerts pleiotrophic effects in different tissues. For instances, within the vascular-endothelial system, nitric oxide functions as an effective vaso-relaxant [1]. However, when present in the central and peripheral nervous systems, nitric oxide functions as a neurotransmitter [2]. On the other hand, nitric oxide is an antitumoral and antimicrobial defense agent produced by immune and glial cells in the context of mammalian host immunity [3].

With a half-life of only 3–5 sec *in vivo*, nitric oxide can readily enter a cell or move between cells many times within this time span [4] and react with the heme group of guanylate cyclase (GC), triggering a conformational change in GC and the catalysis of guanosine-5′-triphosphate (GTP) to cyclic guanosine 3′,5′-monophosphate (cGMP) [4] and protein phosphorylation. GC activation is believed to be the main nitrergic signal transduction pathway. cGMP acts as a second messenger that activates protein kinase G 1 and 2, with the former involved in intracellular Ca^{2+} control and the latter regulating anionic influx, for example chloride [5, 6]. This transduction pathway can affect a broad range of proteins directly, for example phosphodiesterases of cyclic nucleotides and indirectly, for example protein kinase A, thus increasing the level of adenosine 3′,5′-monophosphate (cAMP) with activation of proteins involved in the cAMP downstream pathway [7, 8].

Nitric oxide is capable of affecting other cellular signalling pathways independent of GC activation. As nitric oxide is thermodynamically unstable, it is able to undergo various chemical reactions with gaseous molecules, anions and reactive oxygen species (ROS) to form nitrites, nitrates and peroxynitrites ($ONOO^-$). Nitric oxide reacts quickly with the superoxide anion ($O_2{\bullet}^-$) to form peroxynitrite ($ONOO^-$) to avoid its elimination by the antioxidant systems. $ONOO^-$ has an action radius of 100 μm and even shorter of half-life of 1–2 sec, tending to generate multiple toxic products in its degradation [9]. During the process of these chemical reactions, intermediate products such as (ROS) and other free radicals are produced. These nitrergic intermediate and end-products can induce modifications of lipids, proteins and DNA through oxidation [10], nitration [11] or nitrosylation [12].

The involvement of diverse functional nitric oxide in the nervous system continues to attract researchers' attention as its implication in various neurodegenerative disorders linked to oxidative stress, including ischaemia [13], amyotrophic lateral sclerosis [14], Alzheimer's disease (AD) [15] and Parkinson's disease (PD) [16]. The bi-phasic role of nitric oxide either as a physiological neuromodulator or a neurotoxic factor is dependent on the level of intracellular nitric oxide. Nitric oxide induced cytotoxicity is significantly elevated in pathological conditions implicating the generation of ROS and $ONOO^-$ as a key mechanism in brain injury where

they are both likely to mediate programmed cell death (PCD) [17, 18]. Moreover, iNOS induction by diverse stimuli such as endotoxins or cytokines and during excitotoxicity caused by constitutive activation of glutamate receptors can result in overproduction of nitric oxide because of increased nNOS activity [19]. Chronic $A\beta_{1-40}$ intracerebroventricular infusion in an AD model has been demonstrated to induce $ONOO^-$ formation resulting in nitration of tyrosyl residues of proteins [20]. In ischaemia/reperfusion and stroke models, the higher nitric oxide level is accounted for by increased synthesis activity of iNOS and the constitutive isoforms of NOS triggered by elevated Ca^{2+} level [21]. However, the role of nitric oxide in ischaemia remains controversial. Inhibition of nitric oxide production in iNOS and nNOS knockout mice or by non-selective pharmacological inhibitor has demonstrated neuroprotective effects in models of cerebral ischaemia [22] and traumatic brain injury [23], respectively. On the contrary, [24] demonstrated that pre-treatment with NOS inhibitor aggravated neuronal death whereas post-treatment showed no neuronal rescue effect on cerebral ischaemia injury. In PD, inhibition of parkin [25] and glutathione reductase [26] activities by $ONOO^-$-induced protein modification increased susceptibility to neuronal death as a result of lower cellular antioxidant defense.

As nitric oxide has widespread implications in the pathogenesis of numerous neurodegenerative diseases because of its toxic and undesirable interaction with ROS, an understanding of the mechanisms of nitric oxide mediated neuronal injury provides a screening platform for identification of potential universal biological targets involved in neuronal death. Our current study of the neuronal transcriptome revealed a stunning list of 3672 probe sets exhibiting transcriptional regulation of at least ± 1.5-fold change in a minimum of one out of three time-points (8, 15 and 24 hrs) in nitric oxide mediated neuronal injury. Biological functional annotation of these genes revealed that multiple enriched biological processes were significantly regulated. Although some of these over-represented pathways have been documented to a degree, many are novel providing unique insights into nitric oxide related neuronal injury, enabling us to define the temporal profile of recruitment of death signalling.

Materials and methods

Materials

Neurobasal™ (NB) medium, B-27 and GlutaMAX supplements were from Invitrogen/GIBCO™ (Carlsband, CA, USA). Cell culture plates were from NUNC (Naperville, IL, USA). NOC-18 (DETA-NONOate, (*Z*)-1-[2-(2-Aminoethyl)-*N*-(2-ammonioethyl)amino]diazen-1-ium-1,2-diolate from Alexis Biochemical (San Diego, CA, USA). The primary antibodies used in Western blot analysis were as follows: active caspase-3 antibody from BD Biosciences PharMingen (San Diego, CA, USA); α-fodrin antibody from

Chemicon (Temecula, CA, USA) and β-tubulin antibody from Cytoskeleton (St. Denver, CO, USA). All other nutrients, salts and antibiotics used in the culture media or assay buffers were from Sigma (Singapore).

Cell culture preparation for murine primary cortical neurons

The primary cultures were prepared by using neocortical neurons (gestational days 15 or 16) obtained from foetal cortices of Swiss albino mice following previous described procedures with modifications [27]. Microdissected cortices were subjected to trypsin digestion and mechanical trituration. Cells were collected by centrifugation and resuspended in NB medium containing 2.5% B-27 supplement, 1% penicillin, 1% streptomycin, 0.25% GlutaMAX-1 supplement and 10% dialysed foetal calf serum. Twenty-four well plates previously coated with poly-D-lysine (100 μg/ml) were seeded with cells at a density of 2×10^5 cells/cm^2 and used for subsequent experiments. The cultures were maintained at 37°C overnight in a humidified 5% CO_2 and 95% air incubator and the culture media changed to a serum-free NB medium containing all previously mentioned constituents. Immunocytochemical staining for microtubule-associated protein-2 and glia fibrillary acidic protein revealed more than 95% of the cells in day 5 *in vitro* cultures were neurons with minimal contamination by glia [27]. All experiments involving animals were approved by the National University of Singapore (Protocol no. 727/05) and were in accordance with the Ethical principles and guidelines for scientific experiments on animals' of the Swiss Academy of Medical Sciences.

Drug preparation and treatment

Nitric oxide donor, NOC-18 was prepared as 100 mM aqueous stock solution containing 0.01 M sodium hydroxide (NaOH) and stored at –20°C. On day 7 *in vitro*, the cultured neurons were treated with respective drug in NB medium.

Hoechst stain

Cells were fixed with 4% paraformaldehyde in phosphate buffered saline. Fixed cells were then incubated with Hoechst 33342 at the final concentration of 2 μg/ml. Stained nuclei were observed and analysed under a fluorescence microscope (Leica DM IRB).

Qualitative and quantitative analysis of cell viability

The 3-(4,5-dimethylthiazole-2-yl)-2,5-diphenyltetrazolium bromide (MTT) assay was employed as index of cell survival [27]. MTT was dissolved at a stock concentration of 5 mg/ml in RPMI-1640 medium (GIBCO). Thirty microlitres of MTT solution was added to each well of the 24-well plate containing 300 μl culture medium. After incubation at 37°C for 20 min, the culture medium was removed by aspiration. The formazan formed in the wells was dissolved by an aliquot of 200 μl DMSO and the absorbance of the solution was read using a TECAN plate reader at a wavelength of 570 nm. Results from MTT assay are presented as mean ± S.E.M. from three independent experiments.

Western blotting

Cells were lysed with RIPA buffer (10 mM Tris-HCl, pH 7.4, 1 mM EDTA, 150 mM NaCl, 1% Nonidet-P40, 0.5% deoxycholate, 0.1% SDS, protease inhibitor cocktail tablet) and spun down at $16,000 \times g$ for 10 min to obtain the supernatants whose concentrations were quantitated using Biorad RC-DC assay. Ten micrograms of proteins from individual supernatant samples containing $1 \times$ SDS (with 20% freshly added β-mercaptoethanol) were heated to 100°C for 5 min, cooled down to room temperature and subsequently centrifuged for 2 min at $16,000 \times g$. Equal amount of protein was loaded and subjected to SDS-PAGE (12% gel) and immunoblotted using commercially available antibodies. Antitubulin (1:1000; Cytoskeleton Inc., St. Denver, CO, USA) monoclonal antibody was used for internal control purpose. Antibody-reactive bands were detected using chemiluminescence (Pierce Biotechnology Inc., Rockford, IL, USA) and exposure to x-ray film (Eastman Kodak Company, Rochester, New York, USA).

Total RNA extraction and isolation

RNA from samples was extracted using RNeasy Mini Kit (Qiagen Cat. No. 74104) according to the manufacturer's instructions. All pipette tips used were RNase-free and with filters. The following procedures were suited for 1×10^6 cultured cells per sample. 1.5 μl of the RNA sample was aliquoted for spectrophotometric quantification using Nanodrop ND-1000 Version 3.2.1 and 1 μl for RNA quality analysis using E-gene HDA-GT12 genetic analyser.

Affymetrix microarray using Affymetrix® GeneChip Mouse Genome 430 2.0 array

Microarray analysis was carried out using 14 GeneChip Mouse Genome 430 2.0 array (Affymetrix, Santa Clara, CA, USA), which contain 45,000 probe sets and can analyse the expression level of over 39,000 transcripts and variants from over 34,000 well-characterized mouse genes. The assignment of the arrays (GeneChip) was as follows: vehicle-treated control ($n = 5$); NOC-18-treatment for 8, 15 and 24 hrs NOC-18 treatment ($n = 3$ for each time-point).

According to technical manual form Affymetrix, 7 μg of extracted total RNA was used for cDNA synthesis. Double-stranded cDNA was synthesized using Superscript II reverse transcriptase (Invitrogen, Carlsbad, CA, USA) with a T7-dT24 primer. After cleanup, Biotin-labelled cRNA was synthesized by *in vitro* transcription (Enzo Diagnostic, Inc., NY, USA) and fragmented subsequently. Fifteen micrograms of fragmented cRNA produced above was hybridized to the arrays for 16 hrs at 45°C. The hybridized arrays were washed, stained, and scanned according to the manufacturer's instructions. The data from each array were collected and initially analysed using Affymetrix Microarray Suite 5.0 software. For comparison of multiple arrays, the signal intensity of each array was scaled to 500. The regulated genes were filtered on fold change 1.5-fold against controls in at least one of three time-points. One-way ANOVA ($P < 0.05$) approach was used to find differentially expressed genes using GeneSpring™ GX 7.3 software (Agilent Technologies, CA, USA). Functional information about each gene product was obtained from web-based database NetAffx (3′ IVT Expression, Affymetrix), web-based applications DAVID 2008 (http://david.abcc.ncifcrf.gov/) and from direct searches of the primary literature (PubMed: http://www.ncbi.nlm.nih.gov/pubmed/).
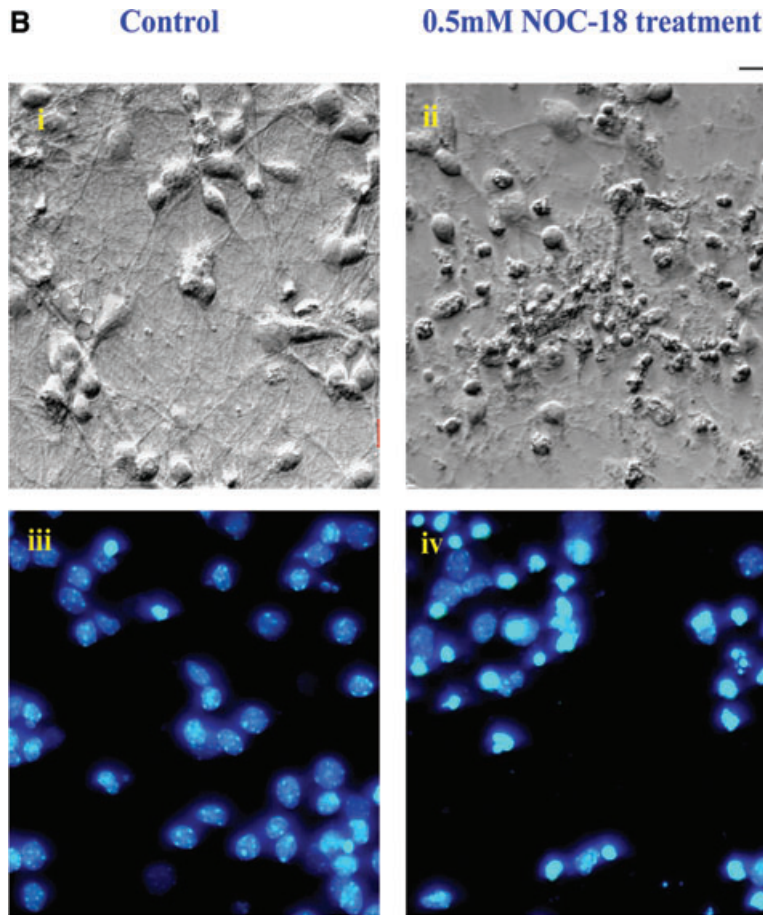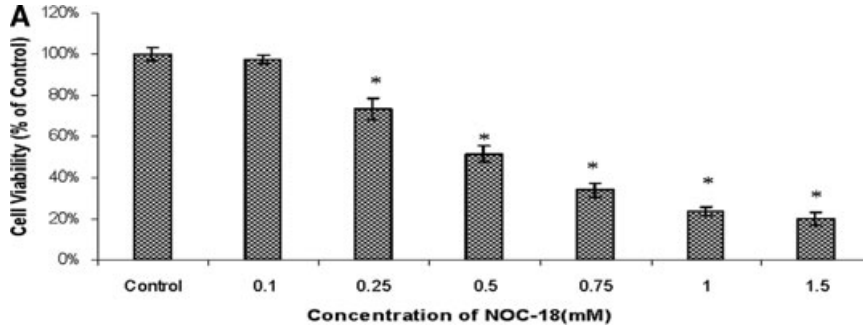
Fig. 1 (**A**) Cell viability assay revealed a dose-dependent increase in neuronal death of NOC-18-treated primary cortical neurons. Day 7 murine primary cortical neurons were treated with NOC-18, A nitric oxide donor, at various concentrations. MTT assay was conducted 24 hrs later. Data are representative of three independent experiments performed in replicates ($^*P < 0.05$ as compared with the control). (**B**) Round shrunken apoptotic bodies with chromatin condensation were observed in nitric oxide induced neuronal injury. Hoffman imaging of control (i) and 0.5 mM NOC-18-treated (ii) primary cortical neurons was performed after 24 hrs post-treatment (Top). Hoechst nuclei stain was subsequently carried out to reveal extent of chromatin condensation in control (iii) and nitric oxide treated (iv) neurons (Bottom). Each scale bar represents 10 μm. Data are representative of three independent experiments.

Microarray bioinformatics analysis

The absolute data (signal intensity, detection call and detection P value) were exported into GeneSpring[tm] GX 7.3 (Agilent Technologies, San Diego, CA, USA) software for analysis by parametric test based on crossgene error model. One-way ANOVA approach was used to identify differentially expressed genes. Array data were globally normalized using GeneSpring software. After per chip normalizations and per gene normalization, genes were filtered on fold change ±1.5-fold against controls in at least one of three conditions. Finally, one-way ANOVA approach

($P < 0.05$) and Benjamini-Hochberg FDR Correction were used to find differentially expressed genes. Genes which were differentially expressed are annotated using Database for Annotation, Visualization, and Integrated Discovery (DAVID) V6.7 (http://david.abcc.ncifcrf.gov/) and PubMed (http://www. ncbi.nlm.nih.gov/pubmed/) search. All microarray data reported here is described in accordance with MIAME guidelines and has been deposited in NCBIs Gene Expression Omnibus (GEO; http://www.ncbi.nlm.nih.gov/geo/) and are accessible through GEO Series accession number GSE22087 for nitric oxide global transcriptomic profile.

Fig. 2 (**A**) Immunoblotting against pro- and active caspase-3 revealed caspase-3 activation at 15 hrs after 0.5 mM NOC-18 treatment. Pro-caspase-3, a 32 kD pro-enzyme is cleaved into two functional subunits of 17 and 11 kD, respectively, to form the active caspase-3 complex. (**B**) Immunoblotting against α-fodrin demonstrated simultaneous caspase-3 and calpains activation at 15 hrs after 0.5 mM NOC-18 treatment. α-Fodrin, a common substrate to both caspase-3 and calpains, is cleaved to 120 kD and 145/150 kD protein fragments upon caspase-3 and calpains activation, respectively. Initial expression of the 120 and 145/150 kD occurred at 15 hrs post-NOC-18 treatment on murine primary cortical neurons. Cultured neurons were treated with 0.5 mM NOC-18 and samples harvested with RIPA buffer from 4 to 24 hrs post-treatment. Ten micrograms of supernatant proteins from individual treatment was loaded in each lane and subjected to SDS-PAGE and immunoblotting analysis. Staurosporine (STA), a broad-spectrum kinase inhibitor, is well known for its role in induction of mitochondrial-dependent caspase-3-mediated neuronal death and is in this case used as a positive control for neuronal treatment at 0.5 μM. Each immunoblot is representative of three independent analyses.
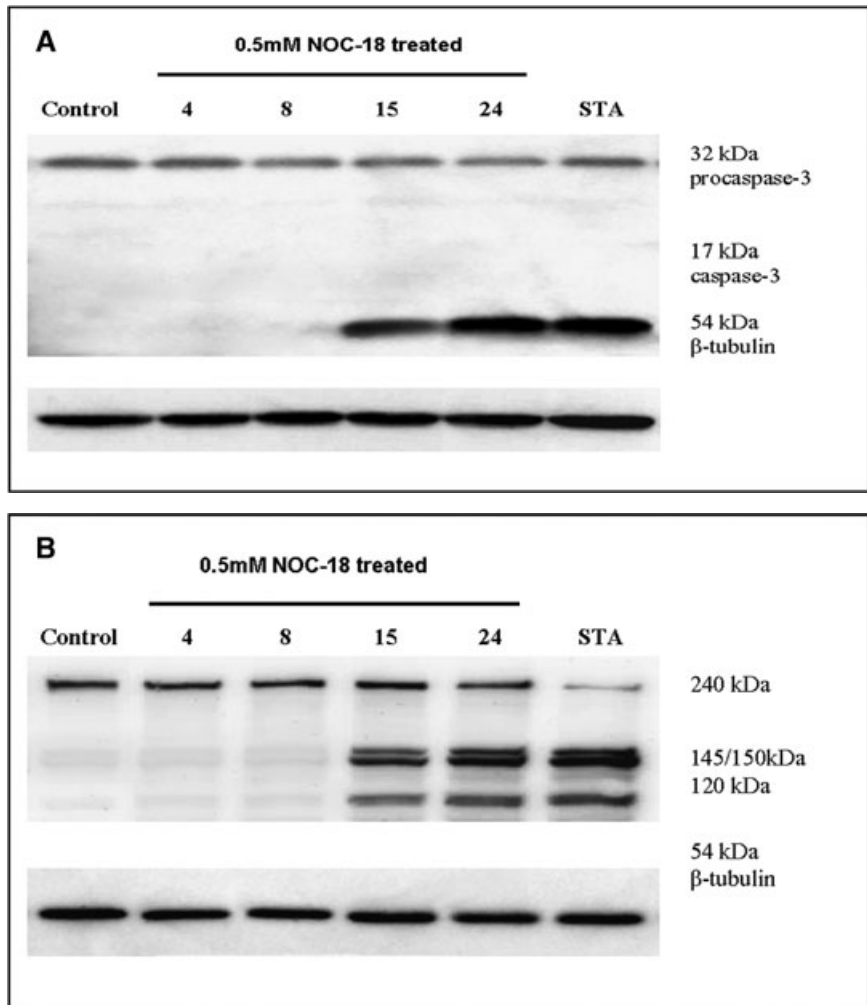
Real-time PCR

Reverse transcription was carried out according to steps specified by manufacturer (Applied Biosystems Taqman reverse transcription reagents). Each cDNA sample was duplicated with two No Template Control (NTC) for each probe used. Twenty microlitres of the Taqman master mix was pipetted to the bottom of each well of the optical 96-well fast reaction plate. Five microlitres of cDNA or water (NTC) was added to the designated reaction well. The plate was then read by the 7000 Fast Real-Time PCR System with conditions according to the manufacturer's protocol.

Statistical analysis

Values are mean $\pm$ S.E.M. of at least three independent experiments. Data were analysed using Tukey test with one-way ANOVA to assess significant differences in multiple comparisons. Values of $P < 0.05$ were considered as statistically significant and presented as mean $\pm$ S.E.

Results

Nitric oxide induced apoptotic cell death in cultured primary neurons

High doses of nitric oxide, frequently observed in the pathogenesis of neurodegenerative disease, cause neuronal death. In this study, we adopt a neuronal model of cultured day 7 murine primary cortical neurons. Cell viability assay demonstrated a concentration-dependent decrease in cell viability after 24 hrs treatment with NOC-18 (a nitric oxide donor; Fig. 1A). As determined from Figure 1A, the IC_{50} for nitric oxide was 0.5 mM (51.2 $\pm$ 4.0% cell viability). Morphological analysis of 0.5 mM NOC-18-treated neurons by Hoffman modulation contrast imaging demonstrated cell shrinkage into round apoptotic cell bodies with absence of neuritic outgrowths and [Fig. 1B(ii)] when compared to the healthy control neurons [Fig. 1B(i)]. There was an absence of rapid swelling indi-
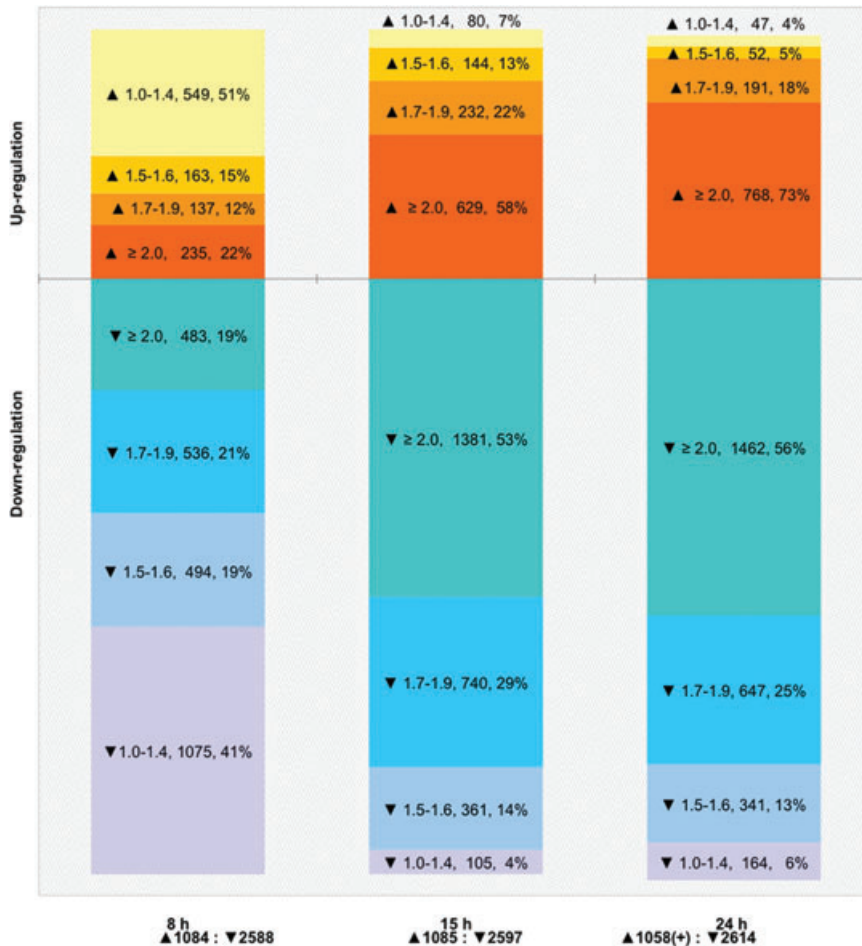
Up-regulation

▲ 1.0-1.4, 549, 51%

▲ 1.5-1.6, 163, 15%
▲ 1.7-1.9, 137, 12%

▲ ≥ 2.0, 235, 22%

▲ 1.0-1.4, 80, 7%
▲1.5-1.6, 144, 13%
▲1.7-1.9, 232, 22%

▲ ≥ 2.0, 629, 58%

▲ 1.0-1.4, 47, 4%
▲1.5-1.6, 52, 5%
▲1.7-1.9, 191, 18%

▲ ≥ 2.0, 768, 73%

Down-regulation

▼ ≥ 2.0, 483, 19%

▼ 1.7-1.9, 536, 21%

▼ 1.5-1.6, 494, 19%

▼1.0-1.4, 1075, 41%

▼ ≥ 2.0, 1381, 53%

▼ 1.7-1.9, 740, 29%

▼ 1.5-1.6, 361, 14%
▼ 1.0-1.4, 105, 4%

▼ ≥ 2.0, 1462, 56%

▼ 1.7-1.9, 647, 25%

▼ 1.5-1.6, 341, 13%
▼ 1.0-1.4, 164, 6%

8 h
▲1084 : ▼2588

15 h
▲1085 : ▼2597

24 h
▲1058(+) : ▼2614

Fig. 3 Time-course profiling revealed a significant increase in number of up/down-regulated genes with transcriptional expression ≥twofold change from 8 to 24 hrs timeframe. Only genes with transcriptional fold-change of at least ±1.5 in at least one out of three time-points and had passed stringent statistical analysis (one-way ANOVA, $P < 0.05$) were included into nitric oxide global gene profile (a total of 3672 gene probes). Genes were then segregated into fold-change categories at respective time-points.

cating that accidental necrosis was not involved [18]. In addition, Hoescht stain illustrated the presence of chromatin condensation in these round cell bodies [Fig. 1B(iv)] as opposed to that of control cells [Fig. 1B(iii)], further confirming induction of neuronal death predominantly by apoptotic-like injury by 0.5 mM of NOC-18. In this study, 0.5 mM of NOC-18 was chosen for subsequent time-course experiments.

To understand the nature of nitric oxide induced neuronal injury, immunoblot analysis against inactive pro-caspase-3 (32 kD) and active caspase-3 (made up of a 12 and 17 kD subunits) was conducted. Figure 2A demonstrated a time-dependent increase in caspase-3 activation, with prominent overexpression of the active 17 kD subunit observed after 15 hrs post-treatment. Caspase-3 activation was further confirmed by the presence of the 120 kD truncated α-fodrin fragment from 15 hrs post-treatment (Fig. 2B). Expression of the 145/150 kD α-fodrin protein fragment also suggested the presence of calcium-activated calpains activation in nitric oxide induced neuronal injury (Fig. 2B). These data are suggestive of PCD, which is slow in onset and involves the recruitment of multiple proteases [18].

Gene expression in nitric oxide induced neuronal apoptosis

Affymetrix GeneChip Mouse Genome 430 V2.0 arrays were used to perform the microarray experiment on day 7 murine primary cortical neurons treated with 0.5 mM of NOC-18 over a time-course of 8, 15 and 24 hrs. All differentially expressed genes in this study were selected based on criteria of a minimum of ±1.5-fold change in at least one of three time-points and subjected to statistical testing by one-way ANOVA, $P < 0.05$ and Benjamini-Hochberg False Discovery Rate (FDR) Correction using GeneSpring v7.3 software. FDR, a commonly adopted statistical analysis, controls the proportion of the most relevant errors among those tests whose null hypothesis were rejected.

Out of a total of 45,000 probe sets representing over 34,000 well-characterized mouse genes, 3,672 microarray chip-annotated probe sets were profiled after 0.5 mM NOC-18 treatment (Fig. 3A). As demonstrated in Figure 3A, the number of down-regulated genes at individual time-points in NOC-18 treatment substantially overwhelmed the up-regulated genes. Across the three time-
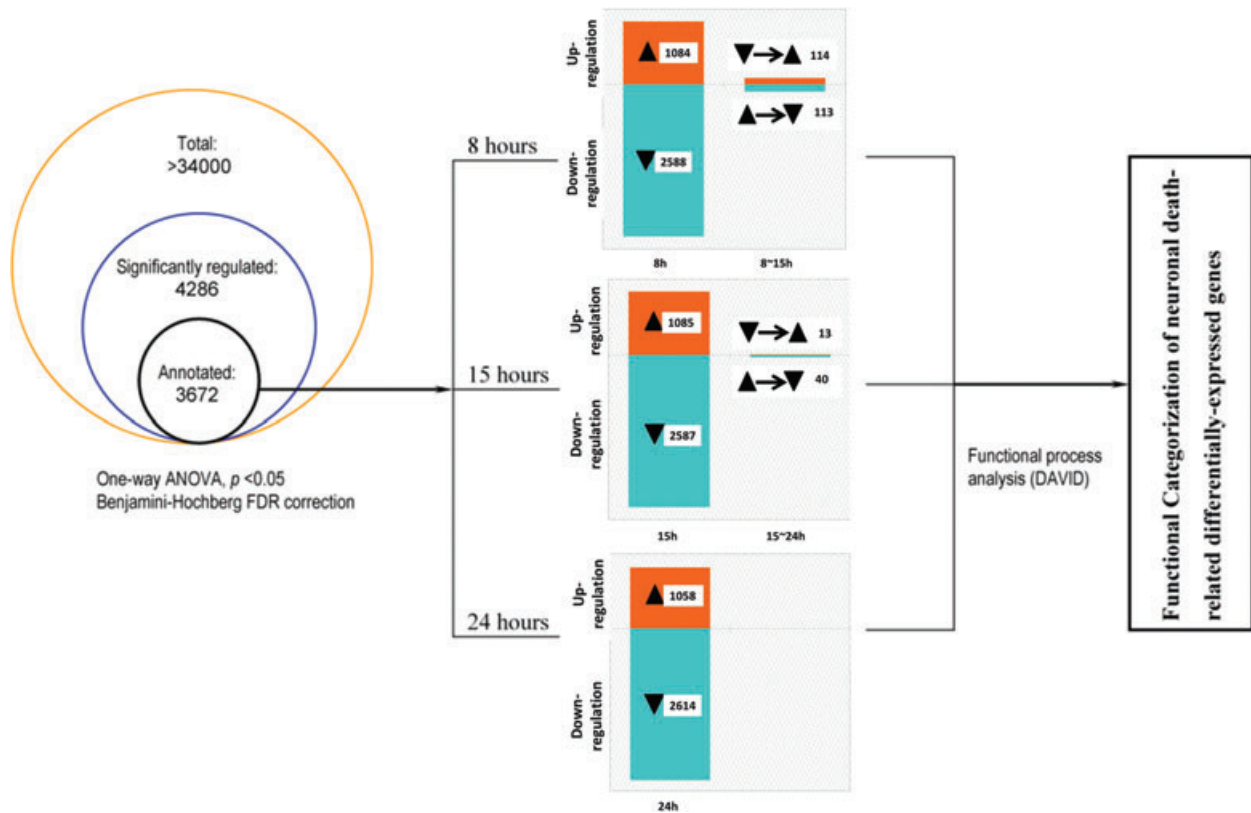
Fig. 4 Flowchart of microarray analyses and profiling of neuronal death-related differentially expressed genes in nitric oxide mediated neuronal injury.

points, close to 30% of total gene probes demonstrated transcriptional up-regulation above the basal level of 1.0-fold. Within these up-regulated gene probes, the number of genes with fold-change difference above 1.5 significantly increases from 49% (8 hrs) to 96% (24 hrs). This tremendous increase was attributed to the expansion of the ≥2-fold change category from the initial 22% (8 hrs) to an escalating 58% (15 hrs), and continued on a slow steady increase to 73% (24 hrs). A similar trend was also observed for the down-regulated gene probes (Fig. 3). As such, it can be inferred that the most significant transcriptional regulation occurred between 8 and 15 hrs.

The global gene profile list representative of NOC-18-mediated neuronal injury (3672 microarray chip-annotated probes sets) was then subjected to functional-gene ontology classification by DAVID 6.7 analysis [28, 29]. DAVID interpretation recognized 3484 biologically and functionally reported genes from various biological databases for nitric oxide treatment (as shown in Fig. 4).

To derive inferences pertaining to the temporal recruitment of cellular pathways and functional processes were altered, we performed a more structured over-representation analyses on the identified genes. The 3484 differentially expressed annotated genes were then classified into time-point-specific up/down-regulated categories based on (1) their fold-change above/below 1.5 at the

specific time-point; and (2) if fold-change at the time-point is between −1.5 and 1.5, the inter-time-point up/down regulatory trend. This is to facilitate the identification of the temporal recruitment and/or activation/inhibition of biological pathways during nitric oxide mediated neuronal injury. To assess if a biological process was statistically significantly enriched, DAVID in-built Expression Analysis Systematic Explorer (EASE) program was employed. It categorizes genes to functional categories within the gene ontology hierarchical database and denotes which categories in the biological process ontology are statistically over-represented by identified genes. A *P* value < 0.05 for a functional category denotes significant overrepresentation, and 0.05 ≤ *P* values ≤ 0.15 were considered borderline significant.

Despite the vast, useful information that DAVID has interpreted from the global gene profile, its structure is inadequate in providing additional associations (*e.g.* cell type and pathway targets). To complicate matter, many annotated genes on the microarray chip have not yet been fully associated with categories in the appropriate gene ontology hierarchies. This would explain the discrepancy in the number of annotated probe sets between the microarray chip (3672) and the DAVID (3484) defined groups. Consequently, we further substantiate the pathway/process analyses with in-depth literature review to identify and include additional clusters of

Table 1 Selected differentially expressed gene profile of neuronal death-related families in cultured day 7 mouse primary cortical neurons treated with 0.5 mM NOC-18

GenBank	Gene title	Symbol	8 hrs	15 hrs	24 hrs
Cell death			▲60, $P = 4.4^{-5}$ ▼ 69, $P = 0.41$	▲ 49, $P = 5.40^{-4}$ ▼ 65, $P = 0.54$	▲ 48, $P = 4.10^{-4}$ ▼ 65, $P = 0.52$
NM_010019	Death-associated protein kinase 2	Dapk2	5.00 ± 0.47	5.05 ± 0.56	2.02 ± 1.05
NM_020581	Angiopoietin-like 4	Angptl4	1.28 ± 0.41	6.28 ± 1.45	2.63 ± 0.57
NM_133810	Serine/threonine kinase 17b (apoptosis-inducing)	Stk17b	1.84 ± 0.34	3.28 ± 0.71	1.97 ± 0.73
NM_054056	PRKC, apoptosis, WT1, regulator	Pawr	1.61 ± 0.34	3.22 ± 0.66	2.32 ± 0.55
NM_013929	SIVA1, apoptosis-inducing factor	Siva1	−1.12 ±0.35	1.95 ± 0.48	2.27 ± 0.55
NM_009754	BCL2-like 11 (apoptosis facilitator)	Bcl2l11	3.04 ± 0.95	4.90 ± 0.78	7.28 ± 1.39
NM_013749	Tumour necrosis factor receptor superfamily, member 12a	Tnfrsf12a	2.86 ± 0.91	10.82 ±0.93	17.99 ± 0.56
NM_146057	Death-associated protein	Dap	−1.22 ±0.32	2.09 ± 0.48	2.28 ± 0.54
NM_019740	Forkhead box O3	Foxo3	1.10 ± 0.31	1.65 ± 0.48	1.82 ± 0.54
NM_019980	LPS-induced TN factor	Litaf	1.23 ± 0.32	1.95 ± 0.48	1.96 ± 0.57
NM_009068	Receptor (TNFRSF)-interacting serine-threonine kinase 1	Ripk1	1.18 ± 0.37	1.50 ± 0.59	1.70 ± 0.56
Cell survival, growth and development			▲ 27, $P = 0.048$ ▼ 47, $P = 0.092$	▲ 49, $P = 0.13$ ▼ 65, $P = 0.10$	▲ 48, $P = 0.20$ ▼ 65, $P = 0.09$
NM_011632	Tnf receptor-associated factor 3	Traf3	1.55 ± 0.42	4.91 ± 0.82	4.45 ± 0.59
NM_011633	Tnf receptor-associated factor 5	Traf5	1.58 ± 0.56	1.12 ± 0.58	1.87 ± 0.63
NM_007566	Baculoviral IAP repeat-containing 6	Birc6	1.01 ± 0.66	1.59 ± 0.66	1.74 ± 0.69
NM_007540	Brain derived neurotrophic factor	Bdnf	3.51 ± 0.32	2.50 ± 0.49	2.05 ± 0.56
NM_010014	Disabled homologue 1 (*Drosophila*)	Dab1	1.74 ± 0.31	2.58 ± 0.48	3.84 ± 0.54
NM_007912	Epidermal growth factor receptor	Egfr	2.57 ± 0.32	3.39 ± 0.65	1.17 ± 0.54
NM_010207	Fibroblast growth factor receptor 2	Fgfr2	2.11 ± 0.31	1.78 ± 0.48	1.40 ± 0.54
NM_184052	Insulin-like growth factor 1	Igf1	2.57 ± 0.43	3.98 ± 0.54	4.69 ± 0.59
NM_010788	Methyl CpG binding protein 2	Mecp2	2.89 ± 0.45	3.94 ± 1.53	4.97 ± 0.60
NM_013613	Nuclear receptor subfamily 4, group A, member 2	Nr4a2	4.40 ± 0.31	4.04 ± 0.75	4.67 ± 0.54
NM_153529	Neuritin 1	Nrn1	1.72 ± 0.31	1.89 ± 0.49	2.05 ± 0.54
NM_013625	Platelet-activating factor acetylhydrolase, isoform 1b, β1 subunit	Pafah1b1	1.32 ± 0.31	1.77 ± 0.48	2.74 ± 0.54
NM_009367	Transforming growth factor-β2	Tgfb2	2.53 ± 0.44	2.15 ± 0.55	1.07 ± 0.63
NM_009715	Activating transcription factor 2	Atf2	1.45 ± 0.31	1.28 ± 0.49	2.25 ± 0.54
NM_139294	Braf transforming gene	Braf	1.33 ± 0.33	1.46 ± 0.49	2.05 ± 0.56
NM_007700	Conserved helix-loop-helix ubiquitous kinase	Chuk	1.09 ± 0.32	2.12 ± 0.48	1.84 ± 0.55
NM_021461	MAP kinase-interacting serine/threonine kinase 1	Mknk1	2.07 ± 1.32	3.95 ± 1.08	2.70 ± 0.88
NM_013672	Trans-acting transcription factor 1	Sp1	1.11 ± 0.31	1.70 ± 0.49	1.75 ± 0.54
NM_010234	FBJ osteosarcoma oncogene	Fos	31.00 ±1.08	21.65 ± 5.39	16.78 ±0.81
NM_008036	FBJ osteosarcoma oncogene B	Fosb	29.07 ±1.36	13.76 ± 4.48	7.25 ± 1.53
NM_010591	Jun oncogene	Jun	8.63 ± 0.34	6.99 ± 1.18	7.48 ± 0.54
NM_008416	Jun-B oncogene	Junb	7.48 ± 0.76	6.07 ± 0.69	3.86 ± 0.54

Continued

Table 1 Continued

GenBank	Gene title	Symbol	8 hrs	15 hrs	24 hrs
Mitotic cell cycle regulation			▲ 35, $P = 1.1^{-5}$ ▼ 51, $P = 6.0^{-4}$	▲ 26, $P = 4.1^{-4}$ ▼ 54, $P = 5.2^{-5}$	▲ 19, $P = 0.14$ ▼ 54, $P = 4.5^{-5}$
NM_023813	Calcium/calmodulin-dependent protein kinase II, delta	Camk2d	2.38 ± 0.35	6.23 ± 0.49	4.76 ± 0.69
NM_009828	Cyclin A2	Ccna2	1.28 ± 0.31	1.73 ± 0.48	−1.70 ± 0.54
NM_172301	Cyclin B1	Ccnb1	1.34 ± 0.33	1.82 ± 0.49	−3.18 ±0.54
NM_009831	Cyclin G1	Ccng1	1.13 ± 0.44	2.55 ± 0.48	4.27 ± 1.07
NM_019937	Cyclin L1	Ccnl1	1.19 ± 0.31	1.94 ± 0.48	1.61 ± 0.54
NM_023223	Cell division cycle 20 homologue (*S. cerevisiae*)	Cdc20	1.05 ± 0.31	1.66 ± 0.57	−1.76 ± 0.55
NM_145436	Cell division cycle 27 homologue (*S. cerevisiae*)	Cdc27	1.32 ± 0.32	1.47 ± 0.48	2.12 ± 0.54
NM_027118	Cell division cycle 2-like 5 (cholinesterase-related cell division controller)	Cdc2l5	2.31 ± 0.44	3.77 ± 0.49	4.34 ± 0.57
NM_009874	Cyclin-dependent kinase 7 (homologue of Xenopus MO15 cdk-activating kinase)	Cdk7	1.12 ± 0.31	1.52 ± 0.48	1.87 ± 0.54
NM_026014	Chromatin licensing and DNA replication factor 1	Cdt1	1.33 ± 0.31	1.83 ± 0.48	2.81 ± 0.56
NM_007862	Discs, large homologue 1 (*Drosophila*)	Dlg1	1.06 ± 0.32	1.39 ± 0.48	1.85 ± 0.54
NM_013642	Dual specificity phosphatase 1	Dusp1	2.13 ± 0.31	2.30 ± 0.48	1.91 ± 0.54
NM_007893	E4F transcription factor 1	E4f1	1.20 ± 0.32	1.65 ± 0.48	2.05 ± 0.54
NM_011808	E26 avian leukemia oncogene 1, 5′ domain	Ets1	1.86 ± 0.49	2.67 ± 0.57	1.95 ± 0.62
NM_183186	Forkhead box N3	Foxn3	1.45 ± 0.32	1.62 ± 0.48	−1.00 ± 0.55
NM_007836	Growth arrest and DNA-damage-inducible 45α	Gadd45a	1.31 ± 0.85	5.09 ± 0.87	9.65 ± 0.80
NM_008655	Growth arrest and DNA-damage-inducible 45β	Gadd45b	3.68 ± 0.35	7.48 ± 0.99	5.72 ± 1.35
NM_011817	Growth arrest and DNA-damage-inducible 45γ	Gadd45g	5.46 ± 0.31	9.09 ± 1.30	8.80 ± 0.54
NM_007569	B-cell translocation gene 1, antiproliferative	Btg1	1.44 ± 0.31	1.95 ± 0.48	1.75 ± 0.55
NM_007570	B-cell translocation gene 2, antiproliferative	Btg2	4.20 ± 0.37	5.75 ± 1.22	6.65 ± 0.96
NM_009770	B-cell translocation gene 3	Btg3	2.96 ± 0.31	5.53 ± 0.84	5.14 ± 0.54
NM_007669	Cyclin-dependent kinase inhibitor 1A (p21)	Cdkn1a	−1.23 ± 0.31	1.73 ± 0.48	2.24 ± 0.54
NM_007670	Cyclin-dependent kinase inhibitor 2B (p15, inhibits CDK4)	Cdkn2b	1.51 ± 0.34	1.85 ± 0.50	1.76 ± 0.63
NM_173378	Transformation-related protein 53 binding protein 2	Trp53bp2	1.24 ± 0.31	1.19 ± 0.48	1.85 ± 0.54
NM_010786	Transformed mouse 3T3 cell double minute 2	Mdm2	−1.03 ± 0.31	1.68 ± 0.48	2.38 ± 0.54
NM_008575	Transformed mouse 3T3 cell double minute 4	Mdm4	1.38 ± 0.36	1.74 ± 0.50	2.63 ± 0.57
NM_001003918	Ubiquitin specific peptidase 7	Usp7	1.31 ± 0.33	1.88 ± 0.48	1.48 ± 0.55
NM_175089	NIMA (never in mitosis gene a)-related expressed kinase 1	Nek1	1.08 ± 0.66	1.58 ± 0.67	1.65 ± 0.77
NM_021606	NIMA (never in mitosis gene a)-related expressed kinase 6	Nek6	1.31 ± 0.31	2.10 ± 0.48	2.39 ± 0.54
NM_010937	Neuroblastoma ras oncogene	Nras	1.08 ± 0.31	1.97 ± 0.48	2.88 ± 0.54
NM_009174	Seven in absentia 2	Siah2	1.60 ± 0.32	1.31 ± 0.49	2.40 ± 0.54
NM_022021	CDK5 and Abl enzyme substrate 1	Cables1	−1.42 ± 0.36	−1.90 ± 0.51	−1.84 ± 0.56
NM_016746	Cyclin C	Ccnc	−1.87 ± 0.32	−2.44 ± 0.49	−5.40 ± 0.55
NM_007631	Cyclin D1	Ccnd1	−2.44 ± 0.31	−1.34 ± 0.48	−1.99 ± 0.55

Continued

Table 1 Continued

GenBank	Gene title	Symbol	8 hrs	15 hrs	24 hrs
NM_009829	Cyclin D2	Ccnd2	−1.79 ± 0.31	−1.38 ± 0.48	−2.44 ± 0.54
NM_009830	Cyclin E2	Ccne2	−2.22 ± 0.34	−1.92 ± 0.49	−2.23 ± 0.55
NM_007634	Cyclin F	Ccnf	−1.21 ± 0.50	−1.96 ± 0.62	−2.13 ± 0.65
NM_023243	Cyclin H	Ccnh	−2.36 ± 0.31	−1.82 ± 0.48	−2.24 ± 0.54
NM_172839	Cyclin J	Ccnj	−1.35 ± 0.32	−1.72 ± 0.48	−2.18 ± 0.54
NM_001045530	Cyclin J-like	Ccnjl	−1.75 ± 0.32	−1.78 ± 0.48	−3.95 ± 0.55
NM_001080818	CDC14 cell division cycle 14 homologue A (*S. cerevisiae*)	Cdc14a	−1.52 ± 0.44	−1.30 ± 0.55	−5.73 ± 0.64
NM_178347	CDC23 (cell division cycle 23, yeast, homologue)	Cdc23	−1.41 ± 0.31	−2.13 ± 0.48	−2.42 ± 0.54
NM_007658	Cell division cycle 25 homologue A (*S. pombe*)	Cdc25a	−1.44 ± 0.32	−1.75 ± 0.49	−3.21 ± 0.54
NM_139291	Cell division cycle 26	Cdc26	−1.43 ± 0.31	−1.81 ± 0.48	−2.36 ± 0.54
NM_025950	Cell division cycle 37 homologue (*S. cerevisiae*)-like 1	Cdc37l1	−1.27 ± 0.32	−1.88 ± 0.48	−1.93 ± 0.55
NM_013538	Cell division cycle associated 3	Cdca3	−1.00 ± 0.32	−1.45 ± 0.49	−8.16 ± 0.54
NM_016756	Cyclin-dependent kinase 2	Cdk2	−1.29 ± 0.32	−1.79 ± 0.49	−2.15 ± 0.55
NM_009873	Cyclin-dependent kinase 6	Cdk6	−1.19 ± 0.32	−1.91 ± 0.48	−3.65 ± 0.54
NM_009874	Cyclin-dependent kinase 7 (homologue of Xenopus MO15 cdk-activating kinase)	Cdk7	−2.10 ± 0.35	−2.56 ± 0.52	−9.89 ± 0.55
NM_172717	Checkpoint with forkhead and ring finger domains	Chfr	−1.12 ± 0.31	−2.17 ± 0.48	−2.03 ± 0.54
NM_010093	E2F transcription factor 3	E2f3	−2.13 ± 0.31	−2.72 ± 0.48	−2.32 ± 0.54
NM_146066	G1 to S phase transition 1	Gspt1	−1.43 ± 0.31	−2.19 ± 0.48	−2.80 ± 0.54
NM_026933	TP53-regulated inhibitor of apoptosis 1	Triap1	−1.38 ± 0.31	−1.93 ± 0.48	−1.55 ± 0.54
Endoplasmic reticulum (ER) stress			▲ 6, $P = 3.2^{-3}$ ▼ 5, $P = 0.44$	▲ 6, $P = 2.2^{-3}$ ▼ 5, $P = 0.42$	▲ 6, $P = 1.9^{-3}$ ▼ 5, $P = 0.42$
NM_009883	CCAAT/enhancer binding protein (C/EBP), β	Cebpb	2.47 ± 0.65	4.10 ± 0.49	3.53 ± 0.55
NM_007837	DNA-damage inducible transcript 3	Ddit3	2.12 ± 0.66	5.75 ± 0.48	7.10 ± 0.79
NM_021451	Phorbol-12-myristate-13-acetate-induced protein 1	Pmaip1/Noxa	2.66 ± 0.33	3.29 ± 0.49	5.63 ± 1.15
NM_133234	Bcl2 binding component 3	Bbc3/Puma	1.18 ± 0.31	3.00 ± 0.49	5.83 ± 1.25
NM_024207	Der1-like domain family, member 1	Derl1	1.07 ± 0.31	1.57 ± 0.48	2.12 ± 0.54
NM_010121	eukaryotic translation initiation factor 2α kinase 3	Eif2ak3	1.44 ± 0.31	1.87 ± 0.48	2.18 ± 0.54
NM_015774	ERO1-like (*S. cerevisiae*)	Ero1l	1.06 ± 0.32	2.09 ± 0.48	2.63 ± 0.54
NM_022331	Homocysteine-inducible, endoplasmic reticulum stress-inducible, ubiquitin-like domain member 1	Herpud1	1.40 ± 0.36	2.28 ± 0.48	3.11 ± 0.54
NM_011644	Transient receptor potential cation channel, subfamily C, member 2	Trpc2	1.81 ± 0.50	1.93 ± 0.57	2.02 ± 0.62
NM_029572	Thioredoxin domain containing 4 (endoplasmic reticulum)	Txndc4	1.15 ± 0.31	1.64 ± 0.48	1.83 ± 0.54
NM_138677	ER degradation enhancer, mannosidase α-like 1	Edem1	−1.66 ± 0.32	−1.91 ± 0.48	−1.55 ± 0.54
Response to oxidative stress			▲ 16, $P = 3.2^{-2}$ ▼ N/A	▲ 16, $P = 1.3^{-2}$ ▼ N/A	▲ 16, $P = 8.3^{-5}$ ▼ N/A
NM_013603	Metallothionein 3	Mt3	1.04 ± 0.31	2.14 ± 0.48	2.07 ± 0.54
NM_008706	NAD(P)H dehydrogenase, quinone 1	Nqo1	1.33 ± 0.38	2.31 ± 0.66	3.03 ± 0.57
NM_011034	Peroxiredoxin 1	Prdx1	1.28 ± 0.31	2.05 ± 0.48	2.08 ± 0.55

Continued

Table 1 Continued

GenBank	Gene title	Symbol	8 hrs	15 hrs	24 hrs
NM_007453	Peroxiredoxin 6	Prdx6	1.07 ± 0.31	2.21 ± 0.48	2.48 ± 0.54
NM_019913	Thioredoxin 2	Txn2	1.11 ± 0.31	1.59 ± 0.48	1.87 ± 0.54
NM_029572	Thioredoxin domain containing 4 (endoplasmic reticulum)	Txndc4	1.15 ± 0.31	1.64 ± 0.48	1.83 ± 0.54
NM_015762	Thioredoxin reductase 1	Txnrd1	1.61 ± 0.37	2.51 ± 0.56	3.40 ± 0.56
NM_011198	Prostaglandin-endoperoxide synthase 2	Ptgs2	8.53 ± 0.77	25.00 ± 7.40	37.22 ± 1.70
NM_010442	Heme oxygenase (decycling) 1	Hmox1	18.03 ± 8.04	67.24 ± 1.05	86.75 ± 8.99
NM_029688	Sulfiredoxin 1 homologue (*S. cerevisiae*)	Srxn1	4.72 ± 1.63	11.32 ± 0.48	12.87 ± 2.58
NM_011847	DnaJ (Hsp40) homologue, subfamily B, member 6	Dnajb6	-1.16 ± 0.53	1.86 ± 0.60	1.86 ± 0.64
NM_007869	DnaJ (Hsp40) homologue, subfamily C, member 1	Dnajc1	2.14 ± 0.41	3.93 ± 1.26	3.11 ± 0.59
NM_010481	Heat shock protein 9	Hspa9	1.18 ± 0.31	1.57 ± 0.48	2.31 ± 0.54
NM_030704	Heat shock protein 8	Hspb8	1.73 ± 0.55	4.65 ± 0.52	4.86 ± 0.58
NM_013863	BCL2-associated athanogene 3	Bag3	2.04 ± 0.36	2.77 ± 0.51	2.07 ± 0.57
NM_009825	Serine (or cysteine) peptidase inhibitor, clade H, member 1	Serpinh1	1.35 ± 0.34	4.77 ± 0.75	4.02 ± 0.54
NM_019794	DnaJ (Hsp40) homologue, subfamily A, member 2	Dnaja2	-1.33 ± 0.31	-1.82 ± 0.48	-2.26 ± 0.54
NM_018808	DnaJ (Hsp40) homologue, subfamily B, member 1	Dnajb1	-1.80 ± 0.31	-2.04 ± 0.48	-1.89 ± 0.54
NM_008300	Heat shock protein 4	Hspa4	-1.00 ± 0.31	-2.27 ± 0.48	-1.89 ± 0.54
NM_178385	Tubulin-specific chaperone c	Tbcc	-1.34 ± 0.34	-2.55 ± 0.49	-3.31 ± 0.55
NM_001033149	Tetratricopeptide repeat domain 9	Ttc9	-1.41 ± 0.31	-2.14 ± 0.48	-1.75 ± 0.54
Ubiquitin mediated proteolysis			▲ 24, $P = 2.3^{-5}$ ▼ 17, $P = 8.9^{-3}$	▲ 21, $P = 1.8^{-4}$ ▼ 36, $P = 4.4^{-7}$	▲ 21, $P = 1.8^{14}$ ▼ 36, $P = 4.1^{-7}$
NM_028288	Cullin 4B	Cul4b	1.23 ± 0.32	1.67 ± 0.48	2.16 ± 0.54
NM_176848	F-box protein 2	Fbxo2	1.32 ± 0.33	2.80 ± 0.48	3.83 ± 0.54
NM_172721	F-box and WD-40 domain protein 8	Fbxw8	3.08 ± 0.60	5.42 ± 1.58	4.86 ± 0.68
NM_026101	Hect domain and RLD 4	Herc4	1.16 ± 0.46	1.37 ± 0.71	1.95 ± 0.60
NM_026557	Ring finger and CHY zinc finger domain containing 1	Rchy1	1.23 ± 0.31	1.76 ± 0.48	2.22 ± 0.54
NM_029438	SMAD specific E3 ubiquitin protein ligase 1	Smurf1	1.22 ± 0.38	3.13 ± 0.61	4.18 ± 0.56
NM_019719	STIP1 homology and U-Box containing protein 1	Stub1	-1.21 ± 0.33	1.38 ± 0.49	1.48 ± 0.55
NM_011965	Proteasome (prosome, macropain) subunit, α type 1	Psma1	1.14 ± 0.37	1.81 ± 0.51	1.64 ± 0.56
NM_011184	Proteasome subunit C8 (Psma3)	Psma3	1.35 ± 0.61	2.13 ± 0.52	2.30 ± 0.61
NM_013585	Proteasome (prosome, macropain) subunit, β type 9 (large multifunctional peptidase 2)	Psmb9	1.52 ± 0.39	2.07 ± 0.52	1.99 ± 0.57
NM_026785	Ubiquitin-conjugating enzyme E2C	Ube2c	1.37 ± 0.31	1.96 ± 0.48	-2.16 ± 0.54
NM_173010	Ubiquitin protein ligase E3A	Ube3a	1.38 ± 0.32	1.79 ± 0.48	2.20 ± 0.54
NM_145400	Ubiquitination factor E4A (UFD2 homologue, S. *cerevisiae*)	Ube4a	1.69 ± 0.67	1.99 ± 0.51	2.17 ± 0.56
NM_177327	WW domain containing E3 ubiquitin protein ligase 1	Wwp1	1.20 ± 0.31	1.67 ± 0.48	1.76 ± 0.54
NM_172712	Ubiquitin-like modifier activating enzyme 6	Uba6	-1.82 ± 0.33	-2.17 ± 0.52	-1.96 ± 0.55
NM_145420	Ubiquitin-conjugating enzyme E2D 1 (UBC4/5 homologue, yeast)	Ube2d1	-1.37 ± 0.31	-2.15 ± 0.48	-1.98 ± 0.54

Table 1 Continued

GenBank	Gene title	Symbol	8 hrs	15 hrs	24 hrs
NM_025356	Ubiquitin-conjugating enzyme E2D 3 (UBC4/5 homologue, yeast)	Ube2d3	−1.23 ± 0.31	−2.38 ± 0.49	−1.80 ± 0.54
NM_025985	Ubiquitin-conjugating enzyme E2G 1 (UBC7 homologue, *C. elegans*)	Ube2g1	−1.46 ± 0.31	−2.15 ± 0.48	−1.91 ± 0.54
NM_016786	Ubiquitin-conjugating enzyme E2K (UBC1 homologue, yeast)	Ube2k	−1.30 ± 0.33	−3.11 ± 0.49	−1.51 ± 0.55
NM_027315	Ubiquitin-conjugating enzyme E2Q (putative) 1	Ube2q1	−1.79 ± 0.31	−2.76 ± 0.48	−3.48 ± 0.54
NM_133907	Ubiquitin protein ligase E3C	Ube3c	−1.47 ± 0.31	−1.90 ± 0.48	−1.73 ± 0.54
NM_080562	U box domain containing 5	Ubox5	−2.08 ± 0.33	−2.57 ± 0.51	−2.82 ± 0.55
Glutathione metabolism			▲ 5, $P = 0.06$ ▼ N/A	▲ 12, $P = 1.1^{-4}$ ▼ N/A	▲ 5, $P = 0.04$ ▼ N/A
NM_008160	Glutathione peroxidase 1	Gpx1	1.29 ± 0.32	1.89 ± 0.48	1.69 ± 0.54
NM_010344	Glutathione reductase	Gsr	1.29 ± 0.31	2.18 ± 0.48	3.49 ± 0.75
NM_008180	Glutathione synthetase	Gss	1.25 ± 0.43	3.19 ± 0.48	4.54 ± 0.54
NM_008182	Glutathione S-transferase, α1	Gsta1	2.69 ± 1.32	10.45 ± 0.58	32.10 ± 7.71
NM_008182	Glutathione S-transferase, α2 (Yc2)	Gsta2	2.66 ± 0.71	8.68 ± 0.79	26.73 ± 9.86
NM_010357	Glutathione S-transferase, α4	Gsta4	1.46 ± 0.34	5.78 ± 0.48	11.58 ± 1.15
NM_010358	Glutathione S-transferase, mu 1	Gstm1	1.21 ± 0.31	2.86 ± 0.48	3.27 ± 0.54
XM_904332	Glutathione reductase, mitochondrial precursor (GR) (GRase)	LOC630729	1.47 ± 0.36	2.15 ± 0.48	3.39 ± 0.54
NM_019946	Microsomal glutathione S-transferase 1	Mgst1	1.09 ± 0.31	2.65 ± 0.48	2.47 ± 0.54
Nitric oxide metabolism			▲63, $P = 1.3^{-6}$ ▼45, $P = 0.22$	▲ 21, $P = 0.31$ ▼ 44, $P = 0.23$	▲19, $P = 0.42$ ▼ 44, $P = 0.22$
NM_007494	Argininosuccinate synthetase 1	Ass1	2.39 ± 0.42	4.16 ± 0.60	8.57 ± 1.56
NM_013463	Galactosidase, α	Gla	1.73 ± 0.32	3.33 ± 0.48	2.76 ± 0.54
NM_145953	Cystathionase (cystathionine gamma-lyase)	Cth	1.44 ± 0.51	2.66 ± 0.49	3.25 ± 0.54
NM_008131	Glutamate-ammonia ligase (glutamine synthetase)	Glul	−1.08 ± 0.31	1.61 ± 0.48	−1.41 ± 0.54
NM_013614	Ornithine decarboxylase, structural 1	Odc1	1.35 ± 0.31	1.87 ± 0.48	2.18 ± 0.54
NM_008987	Pentraxin-related gene	Ptx3	1.79 ± 0.32	2.68 ± 0.48	1.63 ± 0.54
NM_013646	RAR-related orphan receptor α	Rora	1.78 ± 0.34	2.74 ± 0.66	2.94 ± 0.55
NM_023141	Torsin family 3, member A	Tor3a	1.71 ± 0.38	1.64 ± 0.52	1.81 ± 0.57

Numerical value after ▲ / ▼ indicates gene count up or down-regulated respectively at designated time-point, and P corresponds to modified Fisher's exact P value, EASE Score; the smaller the more enriched; usually P value is equal or smaller than 0.05 to be considered strongly enriched in the annotation categories. Default set for EASE Score Threshold (maximum probability is 0.1). All fold-change expressions are subjected to one-way ANOVA analysis and significant at $P < 0.05$. Data are expressed as fold-change ± S.E.

genes with known pathway associations in either the identified DAVID gene-ontology categories or the comprehensive identified-gene lists that were not found by the analyses. The overall approach to derive inferences from global gene profiles has been previously documented in several microarray articles [30–32].

In this study, we focus on the over-represented biological processes (with EASE-determined $P < 0.05$) induced in nitric oxide mediated neuronal injury (Table 1) and some of which are listed later. For the purpose of clear distinction during reference to proteins and genes, gene symbols in the text are in italics.

Cell death

A significant number of cell death cascade-related genes demonstrated increase in gene expression which were altered from as early as 8 hrs (Table 1). Genes such as *Dapk2*, *Bcl2l11* and *Tnfrsf12a* demonstrated significant up-regulation at early 8 hrs nitric oxide post-treatment, with maintenance of consistently increasing expression throughout the time-course. Gene candidates potentially up-regulated from 15 hrs composed of *Angptl4, Dap* and *Ripk1*.

Cell survival

Cellular survival-promoting protein-encoding genes, particularly growth factors, for example *Bdnf*, *Igf1* and *Tgfb2* and their receptors, for example *Egfr* and *Fgfr2* showed elevated gene expression at early 8 hrs. To complicate matters, genes critical in neuronal regeneration after injury, such as *Nrn1* and *Nr4a2* also demonstrated an early increase in gene expression. Simultaneous transcriptional elevation also occurred to the tumour necrosis receptors associated factors (Trafs), for example *Traf3* and *Traf5*, pro-survival signalling molecules negatively regulated downstream of *Pawr*. Transcription factors such as FBJ osteosarcoma oncogene (*Fos* and *Fosb*) and Jun oncogene (*Jun* and *Junb*) which target pro-survival genes demonstrated substantial transcriptional up-regulation at 8 hrs.

Mitotic cell cycle regulation

As demonstrated in Table 1, several genes involved in cell cycle progression such as the cyclins (*Ccna2, Ccnb1, Ccng1* and *Ccnl1*) cell division cycle homologues (*Cdc20, Cdc27* and *Cdc2l5*) and cyclin-dependent kinase (*Cdk7*) were mostly highly up-regulated at 15 hrs time-point. Simultaneously, most of the genes encoding for other subtypes of cyclins and cyclin-dependent kinases (Cdks) demonstrated significant persistent decrease in gene expression. On the contrary, genes that encode for proteins involved in the impediment of cell cycle progression, particularly from those of the p53-dependent pathway, such as *Trp53bp2*, *Gadd45a*, *Gadd45b*, *Gadd45g*, *Cdkn1a*, *Cdkn2b* and p53 endogenous inhibitor, *Mdm2* gene expression showed an up-regulation to counteract cell cycle re-activation.

Endoplasmic reticulum stress

A significant transcriptional elevation of severe endoplasmic reticulum (ER) stress-induced pro-apoptotic genes was observed in nitric oxide mediated neuronal injury. These genes composed of *Ddit3*, *Cebpb* and *Pmaip1*, which were highly up-regulated at 8 hrs, and *Bbc3*, *Derl1*, *Herpud1*, *Ero1l* and *Trpc2* at 15 hrs NOC-18 post-treatment as shown in Table 1.

Calcium homeostasis and binding

With the activation of the calcium-dependent calpains (Fig. 2B), it was worthy to examine the regulatory trend of genes encoding for proteins involving in calcium ion homeostasis. Genes encoding for proteins involved in calcium homeostasis and binding were significantly up-regulated in nitric oxide mediated neuronal injury at 8 hrs (Table 1). Examples of these genes include *S100a1*, *S100a4*, *Anxa3*, *AnxA5*, *Fkbp9* and *Fkbp10*.

Response to oxidative stress

In response to the cellular oxidative stress, antioxidant pathways were triggered perhaps in an attempt to rescue to the neuron from oxidative stress-related cell death. These genes consisted of *Ptgs2*, *Hmox1* and *Srxn1*, which were up-regulated at 8 hrs and *Mt3*, *Nqo1* and peroxiredoxins (*Prdx1* and *Prdx6*) at 15 hrs. Furthermore, a handful of genes that encodes for chaperone proteins to alleviate cellular stress in response to aberrant protein formation were induced at 15 hrs in nitric oxide mediated neuronal injury (Table 1). These genes composed of *Dnajb6* and *Dnajc1* (*Hsp40*), *Hspa9* (*Hsp70*), *Hspb8* (*Hsp22*) and *Serpinh1* (*Hsp47*).

Ubiquitin-mediated proteolysis

As nitric oxide is able to trigger protein modifications, it is important to ensure functionality of the ubiquitin–proteasome system (UPS) to perform the necessary protein clearance to reduce aberrant protein buildup. A significant proportion of UPS-related genes underwent significant and vast transcriptional regulation in nitric oxide mediated neuronal injury. Most ubiquitin-conjugating enzymes involved in ligation of ubiquitin protein/polypeptide destined for degradation (*e.g. Ube2c*, *Ube2d1*, *Ube2g1* and especially *Ube2q*) were significantly down-regulated, whereas others (*e.g.* ubiquitin ligases: *Siah2*, *Smurf1* and *Ube3a*) demonstrated transcriptional up-regulation. However, genes encoding for proteasome subunits *Psma1*, *Psma3* and *Psmb9* still demonstrated elevated gene expression. Time-point-specific statistical analyses using modified Fisher's exact *P* value demonstrated a statistical significant suppression of gene expression among UPS members, an indication of UPS dysfunction.

Glutathione metabolism

Consistent with reports that glutathione (GSH) showed neuroprotective against nitrergic neuronal injury through sequestration of nitric oxide by formation of nitrosoglutathione (GSNO), remarkably increases in transcriptional expression of GSH metabolism related proteins (*e.g. Gpx1*, *Gsr*, *Gsta1*, *Gsta2* and *Gsta4*) were observed and documented in nitric oxide global gene profile.
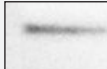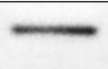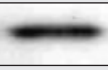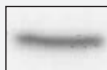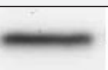
Nitric oxide metabolism

Genes encoding for proteins participating in nitric oxide involved multistep metabolic pathways such as urea cycle (*Ass1*, *Gla*, *Ptx3* and *Tor3a*) were highly up-regulated from the early 8 hrs time-point.

Validation of microarray analysis

Microarray data were validated *via* Western blotting and real-time PCR and indicated a high degree of reliability and specificity.

Table 2 Immunoblotting validation of microarray data performed on 24 hrs 0.5 mM NOC-18-treated murine primary cortical neuron culture

Gene title	Gene symbol	Gene expression (microarray)	Protein expression (Western blot)		
			Control	Treated	
Annexin A3	Anxa3	10.3 ± 1.3			37 kD
Cyclin D1	Ccnd1	−2.0 ± 0.5			36 kD
Cell division cycle 25 homologue A (*S. pombe*)	Cdc25a	−3.2 ± 0.5			65 kD
Heat shock 70 kD protein 8 Heat shock 70 kD protein 9 Heat shock 70 kD protein 14	Hspa8 Hspa9 Hspa14	9.2 ± 0.8 2.3 ± 0.5 2.1 ± 0.5			70 kD
Serine (or cysteine) peptidase inhibitor, clade H, member 1 (47 kD heat shock protein)	Serpinh1 (HSP47)	4.0 ± 0.5			47 kD
		β-Tubulin (internal control)			54 kD

Gene regulation expressed as fold-change ± S.E. Each immunoblot is representative of three independent experiments. Densitometric analysis chart (above) further illustrated the correlation between protein expression and transcriptional expression.

Table 3 Real-time PCR-based validation of microarray data on 24 hrs 0.5 mM NOC-18-treated murine primary cortical neurons

GenBank	Gene title	Symbol	Microarray (24 hrs)	Real-time PCR (24 hrs)
NM_020581	Angiopoietin-like 4	Angptl4	2.63 ± 0.57	4.56 ± 0.69
NM_007837	DNA-damage inducible transcript 3	Ddit3	7.10 ± 0.79	5.05 ± 0.70
NM_011817	Growth arrest and DNA-damage-inducible 45γ	Gadd45g	8.80 ± 0.54	14.64 ± 0.75
NM_010442	Heme oxygenase (decycling) 1	Hmox1	86.75 ± 8.99	61.54 ± 1.67
NM_030704	Heat shock protein 8	Hspb8	4.86 ± 0.58	4.73 ± 0.98
NM_011198	Prostaglandin-endoperoxide synthase 2	Ptgs2	37.22 ± 1.70	36.84 ± 0.87

Data are expressed as fold-change ± S.E. Each real-time PCR probe data is representative of three independent replicates.

Immunoblot analyses (Table 2) and real-time PCR data (Table 3) both confirmed the differential expression profile induced by 0.5 mM NOC-18 treatment.

Discussion

The global gene profiling in this study reflects the simultaneous transcriptional activation and/or inhibition of multiple signalling cascades in nitric oxide mediated neuronal injury wherein 3672 probe sets demonstrated at least ±1.5-fold change in a minimum of one of three time-points (8, 15 and 24 hrs). These data provides an overview of the multi-interactive functions of nitric oxide with induction and inhibition various signalling pathways during the course of its induction of neuronal death. We found recruitment of several biological processes, including apoptotic cell death, survival, cell cycle, ER stress, antioxidative stress response, energy production, ubiquitin-mediated proteolysis, GSH and nitric oxide metabolism. As demonstrated in our study, the final neuronal decision to undergo cell death or survival is determined by the net coordinated effect between the pro- and antiapoptotic proteins. The evidence from our study further confirms the role that nitric oxide plays in the exacerbation of neuronal injury, thus highlighting the importance of its contribution to the pathogenesis of several neurodegenerative diseases where severe cellular oxidative stress is frequently experienced [19]. An understanding of the multiple mechanisms of nitric oxide mediated neuronal
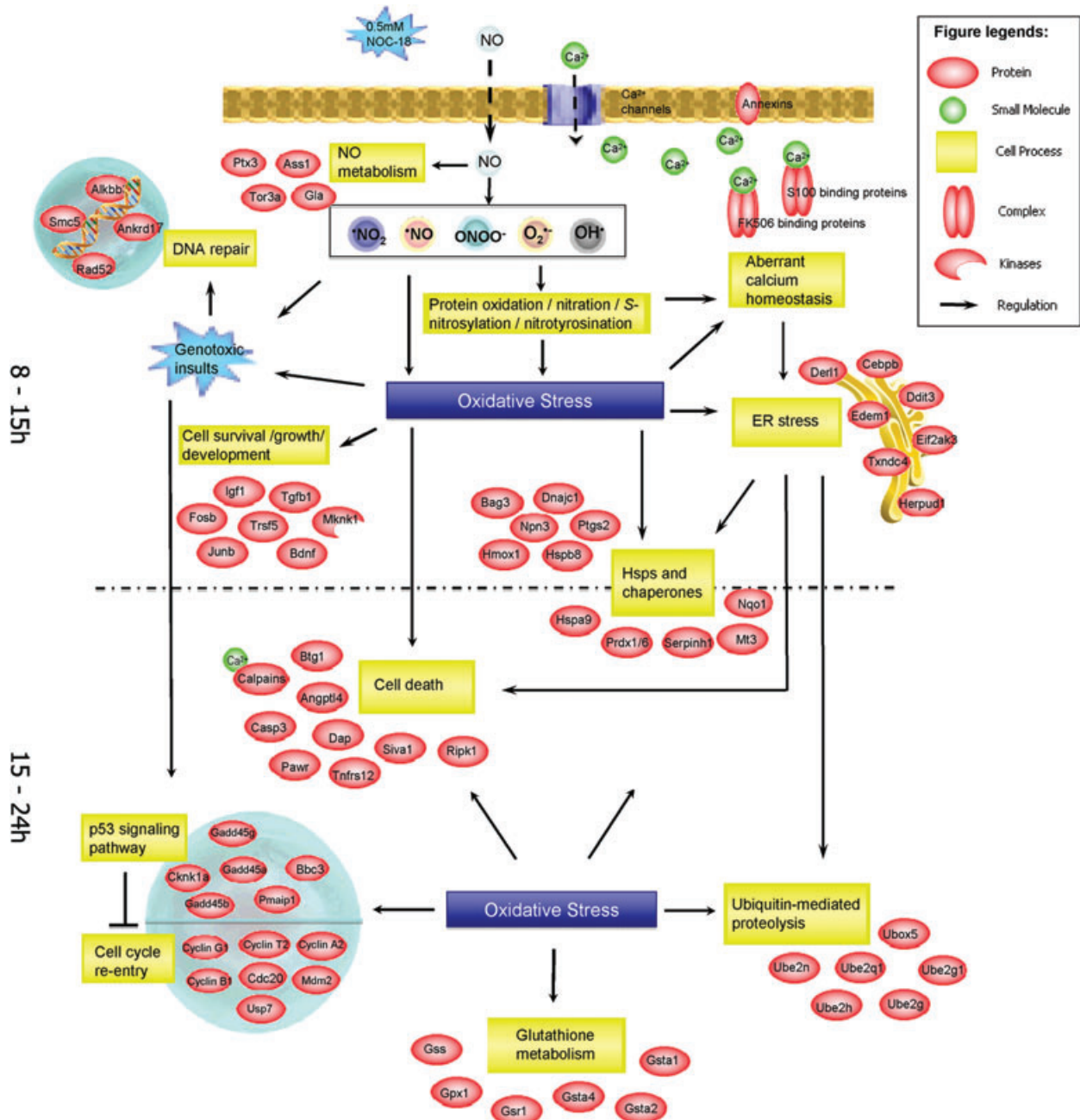
Fig. 5 Time-course analysis of nitric oxide global gene profile demonstrates the sequential activation and/or inhibition of the respective cellular signalling cascades upon nitric oxide entry into the neuron in nitric oxide mediated neuronal injury.

injury is advantageous for the better identification of potential biological targets in the intervention of neurodegenerative disease progression. Indeed, we have been able to provide major insights towards such a goal, including the revelation of the major cellular mechanisms contributing to the nitrergic neuronal injury and their temporal patterns of recruitment.

Time-course of gene profiling in relationship to cellular signalling

Based on temporal recruitment of over-represented biological processes, we are able to postulate an overview of nitric oxide

induction of neuronal death formulated upon the temporal pattern of transcriptomic changes (Fig. 5).

Early- and medium-term events *(8–15 hrs processes)*

(1) Nitric oxide, a membrane-permeable gas diffuses through the cellular membrane.

(2) (a) Because of its excess presence, the nitric oxide metabolic pathways such as the urea cycle are activated in an attempt to remove the exogenous nitric oxide. Evident from the transcriptomic profile of nitric oxide mediated neuronal injury, the *Ass1* gene which encodes for arginosuccinate synthase 1 in the urea cycle for removal of excess nitric oxide, was especially up-regulated at the early 8 hrs time-point. (b) Simultaneously, because of its thermodynamic instability, nitric oxide interacts with other cellular gaseous molecules or ROS to form highly reactive free radicals and nitrergic free radical species ($\bullet NO_2$, $\bullet NO$ and $ONOO^-$).

(3) These radicals and ions induced genotoxic damage and protein modifications, leading to increase oxidative stress. (a) Further, oxidative stress-mediated homeostatic ionic imbalance leads to increase Ca^{2+} cytosolic influx from intra- and extracellular compartments. In fact, perturbed Ca^{2+} ion homeostasis is obvious from nitric oxide transcriptomic profile with increase in gene expression of Ca^{2+}-dependent proteins including pro-apoptotic serine/threonine kinase *Dapk2* (Table 1: Cell death), annexins and *S100* and *FK506* calcium binding proteins. This finding implies an occurrence of excitotoxic event with an increase in intracellular Ca^{2+} level, leading to activation of Ca^{2+}-activated proteins such as calcineurin and calpains (Fig. 2), which mediated cleavage of α-fodrin to 145/150 kD fragments.

(4) Electrophilic stress together with abundant presence of misassembled proteins in ER lumen, converged to ER stress. Also known as ER-associated degradation (ERAD), this system governs ubiquitin-dependent degradation of misfolded ER proteins mediated by ER proteins. Derl1, Herpud1 and Edem1 are ER stress-inducible proteins involved in ERAD which demonstrated significant elevated gene expression at 15 hrs post-treatment in nitric oxide mediated neuronal injury. Nitric oxide mediated ER stress is also prominent from the substantial increase in gene expression of ER stress-responsive pro-apoptotic genes particularly DNA-damage inducible transcript 3 (*Ddit3*), CCAAT/enhancer binding protein (*Cebpb*), phorbol-12-myristate-13-acetate-induced protein 1 (*Pmaip1*), Bcl2-binding component 3 (*Bbc3*; Table 1: ER stress). (C/EBP) β, which was highly up-regulated at the early 8 hrs NOC-18 post-treatment. Dimerization of Ddit3 protein with its partner, Cebpb protein, forms a repressor complex, which inhibits transcription of survival-promoting genes. Bbc3, also known as p53-upregulated modulator of apoptosis (Puma), together with Pmaip1 (Noxa), are p53-mediated ER stress responsive genes as they encode BH3-only proteins, pro-apoptotic members of the Bcl-2 family required to initiate apoptosis through displacement of Bcl2 and Bcl-xL inhibitory interactions with the pro-apoptotic proteins Bax and/or Bak facilitating mitochon-

drial outer membrane permeabilization and cytochrome *c* release [33].

(5) Cellular stress leads to activation of Hsps and chaperones that work to alleviate the stress and restore homeostasis. It has been reported that nitric oxide can exert antiapoptotic effect through induction of cytoprotective gene expression [34]. As a result, several Hsps and chaperones (*e.g. Hspa9, Hspb8, Bag3* and *Serpinh1*), peroxiredoxins (*Prdx1* and *Prdx6*) and metallochaperone, *Mt3*, demonstrated significant increases in gene expression in nitric oxide mediated neuronal injury with *Ptgs2*, *Hmox1* and *Srxn1* being especially highly up-regulated (Table 1: Response to oxidative stress).

(6) Concomitantly, the pro-survival pathways such as growth factor signalling pathways are activated to promote cell preservation. Several of these genes play multifunctional roles in the antiapoptotic process. Birc6 (also known as Bruce), which demonstrated elevated gene expression from 15 hrs (Table 1: Cell survival), is a trans-Golgi peripheral membrane protein that functions as an effective inhibitor of apoptosis (IAP) by inhibition of caspase activity through its Bir domain [35]. It also contains an intrinsic E2/E3 ubiquitin ligase activity that targets Smac for degradation [35]. Deletion of the C-terminal end of Birc6 including the Bir domain resulted in increased p53 expression and nuclear localization with concomitant activation of mitochondrial-dependent apoptosis [36]. The tumour necrosis factor receptor associated factors (Trafs) were significantly up-regulated at 8 hrs. Traf5 have been reported to be involved in Tnf-induced nuclear factor κB (NF-κB) activation, resulting in increased transcriptional activity of pro-survival genes and subsequent protection from cell death [37].

• **Late events** *(15–24 hrs processes)*

(7) As oxidative stress is further aggravated at the later stages, more Hsps and chaperones are activated. GSH metabolic pathway, the strong mammalian antioxidant signalling cascade, also comes into play. Correspond to genes encoding Hsps and molecular chaperones, members of the GSH pathway including glutathione peroxidase 1 (*Gpx1*), glutathione reductase (*Gsr*) and glutathione S-transferase (*Gst*) also demonstrated extensive up-regulation in nitric oxide mediated neuronal injury from as early as 8 hrs (Table 1: GSH metabolism) furthering validating the early occurrence of oxidative stress imposed by high levels of ROS. *Gst* genes, especially those encoding the α class (*Gsta1*, *Gsta2* and *Gsta4*), were highly up-regulated up to multiple of 10-folds gene expression. Gsts are involved in the detoxification of a wide variety of substrates through conjugation of reduced GSH to the electrophilic centre of the compound *via* a sulfhydryl group. Moreover, the glutathione synthase (*Gss*) involved in GSH biosynthesis also demonstrated elevated gene expression at 15 hrs, a further indication of intense cellular oxidative stress.

(8) As the extent of DNA damages becomes increasingly severe, coupling with strong mitogenic signal transduction to promote cell cycle re-activation, the p53 signalling pathway is

brought into the picture to inhibit cell cycle re-entry and enhance the cell death progression. *In vitro* [38] and *in vivo* [39] studies have shown that terminally differentiated neurons destined for cell death are able to replicate DNA. A study by Kruman *et al.* [40] further confirmed that cell cycle re-activation is a vital component of DNA damage response of post-mitotic neurons that can result in apoptosis. Several cell cycle phase progression genes such as cyclins (*Ccna2, Ccnl1 and Ccnt2*) cell division cycle homologues (*Cdc20, Cdc27, Cdc2l5 and Cdc73*), FBJ osteosarcoma oncogene (*Fos* and *Fosb*) and Jun oncogene (*Jun* and *Junb*) showed significant up-regulation in nitric oxide mediated neuronal injury. However, attempt to revive the cell cycle machinery was counteracted by the activation of the p53 signalling pathway, as evident by gene up-regulation of its binding partner (*Trp53bp2*), growth arrest and DNA damage-inducible (*Gadd45*) family, cyclin B1 (*Ccnb1*) and G1 (*Ccng1*) and cell-dependent kinase inhibitors (*Cdkn1a* and *Cdkn2b*), which were related to cell cycle progression and/or DNA damage response. Cdkn1a, commonly known as p21, is involved in the inhibition of critical Cdks activity by hindering their phosphorylation of downstream cell cycle substrate, thus leading to a blockade of cell cycle progression. Gadd45a, Gadd45b and Gadd45g interact with both Cdk1 and cyclin B1, to induce inhibition of the kinase activity of the Cdk1/cyclin B1 complex upon genotoxic stress resulting in G2/M cell cycle arrest [41].

(9) Oxidative stress results in impairment of the mammalian protein clearance machinery. With the mounting accumulation of aberrant proteins in the ER lumen, ER activates its ERAD response to increase protein turnover *via* the UPS route. As such, it is crucial that the cellular inherent protein clearance pathway is functioning optimally to handle the high rate of protein degradation. We have previously reported the presence of UPS dysfunction in nitric oxide mediated neuronal injury [42]. As shown in Table 1, ubiquitin-mediated proteolysis was impaired with the significant down-regulation of majority of the ubiquitin-conjugating enzymes which are crucial in the preparation of proteins for targeted degradation by the proteasomes.

(10) With the increasing homeostatic imbalance inflicted by the perturbation of various biological processes that is beyond restoration, the neuron triggers the cell death machinery, sending itself to demise. When the relative effect of the pro-death molecules overwhelms that of the pro-survival components, the cell death machinery is triggered *via* the activation of multiple cell death signalling cascades including the mitochondrial-dependent cytochrome *c* mediated signalling pathway [43], p53-mediated apoptotic signalling pathway (discussed in early/medium-term processes) [44], and the Fas pathway.

Conclusion

Our study has for the first time addressed concurrently the multiple signalling mechanisms regulated/affected by nitric oxide in its course of mediation of neuronal death. This global gene profiling represents a novel database in term of the temporal patterns of recruitment of signalling cascade to nitrergic neuronal injury. This global gene profile of nitric oxide mediated neuronal injury provides the very initial phase of screening of potential protein candidates whose gene expression can be inhibited or stimulated to form the basis for therapeutic interventions in several neurodegenerative disorders.

Acknowledgements

Conflict of interest

The authors confirm there are no conflicts of interest.

References

1. **Chan W, Yao X, Ko W, *et al*.** Nitric oxide mediated endothelium-dependent relaxation induced by glibenclamide in rat isolated aorta. *Cardiovasc Res.* 2000; 46: 180–7.

2. **Prast H, Philippu A.** Nitric oxide as modulator of neuronal function. *Prog Neurobiol.* 2001; 64: 51–68.

3. **Xie Q, Nathan C.** The high-output nitric oxide pathway: role and regulation. *J Leukoc Biol.* 1994; 56: 576–82.

4. **Ignarro LJ.** Endothelium-derived nitric oxide: actions and properties. *FASEB J.* 1989; 3: 31–6.

5. **French PJ, Bijman J, Edixhoven M, *et al*.** Isotype-specific activation of cystic fibrosis transmembrane conductance regulator chloride channels by cGMP-dependent protein kinase II. *J Biol Chem.* 1995; 270: 26626–31.

6. **Lau KL, Kong SK, Ko WH, *et al*.** cGMP stimulates endoplasmic reticulum Ca(2+)-ATPase in vascular endothelial cells. *Life Sci.* 2003; 73: 2019–28.

7. **Ono K, Trautwein W.** Potentiation by cyclic GMP of beta-adrenergic effect on Ca^{2+} current in guinea-pig ventricular cells. *J Physiol.* 1991; 443: 387–404.

8. **Whalin ME, Scammell JG, Strada SJ, *et al*.** Phosphodiesterase II, the cGMP-activatable cyclic nucleotide phosphodiesterase, regulates cyclic AMP metabolism in PC12 cells. *Mol Pharmacol.* 1991; 39: 711–7.

9. **Whiteman M, Ketsawatsakul U, Halliwell B.** A reassessment of the peroxynitrite scavenging activity of uric acid. *Ann NY Acad Sci.* 2002; 962: 242–59.

10. **Butterfield DA, Stadtman ER.** Protein oxidation processes in aging brain. *Adv Cell Aging Gerontol.* 1997; 2: 161–91.

11. **Souza JM, Daikhin E, Yudkoff M, et al.** Factors determining the selectivity of protein tyrosine nitration. *Arch Biochem Biophys.* 1999; 371: 169–78.

12. **Stamler JS, Toone EJ, Lipton SA, et al.** (S)NO signals: translocation, regulation, and a consensus motif. *Neuron.* 1997; 18: 691–6.

13. **Cuzzocrea S, Riley DP, Caputi AP, et al.** Antioxidant therapy: a new pharmacological approach in shock, inflammation, and ischemia/reperfusion injury. *Pharmacol Rev.* 2001; 53: 135–59.

14. **Cookson MR, Shaw PJ.** Oxidative stress and motor neurone disease. *Brain Pathol.* 1999; 9: 165–86.

15. **Good PF, Werner P, Hsu A, et al.** Evidence of neuronal oxidative damage in Alzheimer's disease. *Am J Pathol.* 1996; 149: 21–8.

16. **Good PF, Hsu A, Werner P, et al.** Protein nitration in Parkinson's disease. *J Neuropathol Exp Neurol.* 1998; 57: 338–42.

17. **Halliwell B.** Oxidative stress and neurodegeneration: where are we now? *J Neurochem.* 2006; 97: 1634–58.

18. **Nagley P, Higgins GC, Atkin JD, et al.** Multifaceted deaths orchestrated by mitochondria in neurones. *Biochim Biophys Acta.* 2010; 1802: 167–85.

19. **Chabrier PE, Demerle-Pallardy C, Auguet M.** Nitric oxide synthases: targets for therapeutic strategies in neurological diseases. *Cell Mol Life Sci.* 1999; 55: 1029–35.

20. **Tran MH, Yamada K, Nakajima A, et al.** Tyrosine nitration of a synaptic protein synaptophysin contributes to amyloid beta-peptide-induced cholinergic dysfunction. *Mol Psychiatry.* 2003; 8: 407–12.

21. **Gross SS, Wolin MS.** Nitric oxide: pathophysiological mechanisms. *Annu Rev Physiol.* 1995; 57: 737–69.

22. **Iadecola C, Zhang F, Casey R, et al.** Delayed reduction of ischemic brain injury and neurological deficits in mice lacking the inducible nitric oxide synthase gene. *J Neurosci.* 1997; 17: 9157–64.

23. **Cherian L, Hlatky R, Robertson CS.** Nitric oxide in traumatic brain injury. *Brain Pathol.* 2004; 14: 195–201.

24. **Lu YC, Liu S, Gong QZ, et al.** Inhibition of nitric oxide synthase potentiates hypertension and increases mortality in traumatically brain-injured rats. *Mol Chem Neuropathol.* 1997; 30: 125–37.

25. **Chung KK, Thomas B, Li X, et al.** S-nitrosylation of parkin regulates ubiquitination and compromises parkin's protective function. *Science.* 2004; 304: 1328–31.

26. **Barker JE, Heales SJ, Cassidy A, et al.** Depletion of brain glutathione results in a decrease of glutathione reductase activity: an enzyme susceptible to oxidative damage. *Brain Res.* 1996; 716: 118–22.

27. **Cheung NS, Pascoe CJ, Giardina SF, et al.** Micromolar L-glutamate induces extensive apoptosis in an apoptotic-necrotic continuum of insult-dependent, excitotoxic injury in cultured cortical neurons. *Neuropharmacology* 1998; 37: 1419–29.

28. **Dennis G Jr, Sherman BT, Hosack DA, et al.** DAVID: Database for Annotation, Visualization, and Integrated Discovery. *Genome Biol.* 2003; 4: P3.

29. **Huang DW, Sherman BT, Lempicki RA.** Systematic and integrative analysis of large gene lists using DAVID Bioinformatics Resources. *Nature Protoc.* 2009; 4: 44–57.

30. **Blalock EM, Grondin R, Chen KC, et al.** Aging-related gene expression in hippocampus proper compared with dentate gyrus is selectively associated with metabolic syndrome variables in rhesus monkeys. *J Neurosci.* 2010; 30: 6058–71.

31. **Blalock EM, Geddes JW, Chen KC, et al.** Incipient Alzheimer's disease: microarray correlation analyses reveal major transcriptional and tumour suppressor responses. *Proc Natl Acad Sci USA.* 2004; 101: 2173–8.

32. **Rowe WB, Blalock EM, Chen KC, et al.** Hippocampal expression analyses reveal selective association of immediate-early, neuroenergetic, and myelinogenic pathways with cognitive impairment in aged rats. *J Neurosci.* 2007; 27: 3098–110.

33. **Kim H, Tu HC, Ren D, et al.** Stepwise activation of BAX and BAK by tBID, BIM, and PUMA initiates mitochondrial apoptosis. *Mol Cell.* 2009; 36: 487–99.

34. **Hao W, Myhre AP, Palmer JP.** Nitric oxide mediates IL-1beta stimulation of heat shock protein but not IL-1beta inhibition of glutamic acid decarboxylase. *Autoimmunity.* 1999; 29: 93–101.

35. **Bartke T, Pohl C, Pyrowolakis G, et al.** Dual role of BRUCE as an antiapoptotic IAP and a chimeric E2/E3 ubiquitin ligase. *Mol Cell.* 2004; 14: 801–11.

36. **Ren J, Shi M, Liu R, et al.** The Birc6 (Bruce) gene regulates p53 and the mitochondrial pathway of apoptosis and is essential for mouse embryonic development. *Proc Natl Acad Sci USA.* 2005; 102: 565–70.

37. **Tada K, Okazaki T, Sakon S, et al.** Critical roles of TRAF2 and TRAF5 in tumour necrosis factor-induced NF-kappa B activation and protection from cell death. *J Biol Chem.* 2001; 276: 36530–4.

38. **Smith DS, Leone G, DeGregori J, et al.** Induction of DNA replication in adult rat neurons by deregulation of the retinoblastoma/E2F G1 cell cycle pathway. *Cell Growth Differ.* 2000; 11: 625–33.

39. **Yang Y, Geldmacher DS, Herrup K.** DNA replication precedes neuronal cell death in Alzheimer's disease. *J Neurosci.* 2001; 21: 2661–8.

40. **Kruman II, Wersto RP, Cardozo-Pelaez F, et al.** Cell cycle activation linked to neuronal cell death initiated by DNA damage. *Neuron.* 2004; 41: 549–61.

41. **Vairapandi, M, Balliet AG, Hoffman B, et al.** GADD45b and GADD45g are cdc2/cyclinB1 kinase inhibitors with a role in S and G2/M cell cycle checkpoints induced by genotoxic stress. *J Cell Physiol.* 2002; 192: 327–38.

42. **Peng ZF, Chen MJ, Yap YW, et al.** Proteasome inhibition: an early or late event in nitric oxide-induced neuronal death? *Nitric Oxide.* 2008; 18: 136–45.

43. **Brown GC.** Nitric oxide and mitochondrial respiration. *Biochim Biophys Acta.* 1999; 1411: 351–69.

44. **Messmer UK, Ankarcrona M, Nicotera P, et al.** p53 expression in nitric oxide-induced apoptosis. *FEBS Lett.* 1994; 355: 23–6.